Backwards Analysis for Retaining Wall System by Sheet Piles based upon Lateral Wall Displacement in St. Petersburg



K. Okajima
Department of Environmental Science and Technology, Mie University, Japan

T. Tanaka
The Japan Association of Rural Resource Recycling Solutions, Japan

A. Zhussupbekov
Department of Civil Engineering, Eurasian National University, Geotechnical Institute, Kazakhstan

ABSTRACT: A test pit work was carried out in 2007 in the area of the Extension of Mariinsky Theater in St. Petersburg, Russia. A sheet pile cofferdam was applied to the work. In the work large displacement of sheet pile was measured. We analyzed this work by the elasto-plastic FEM in total stress condition. In this study Mohr-Coulomb type yield function and Drucker-Prager type plastic potential were applied to constitutive equation. We decided the cohesion of each soil layer from the geological column and the Young's modulus of the strut and sheet pile not to be able to get the detailed soil parameter and the sheet pile and strut data. For this analysis it was obvious that the ineffective strut became a factor of the measured large displacement of the sheet pile.

1 INTRODUCTON

A test pit work with sheet piles was carried out in 2007 in the area of the extension of Mariinsky Theater in St. Petersburg, Russia. The test pit work was carried out to clarify the behavior of soft soils in St. Petersburg. The location of test pit was selected in an intermediate internal area at a safe distance from the existing buildings. In this work the large displacement of sheet pile was observed by the inclinometer.

We analyzed this work by elasto-perfect plastic FEM in total stress condition. It is normally difficult to obtain the stable limit stress condition by computational method when the rotating failure of the retaining structure occurs (Potts, 2003). There are few effective numerical methods to be able to solve this problem. We developed the elasto-plastic finite element analysis with the implicit-explicit dynamic relaxation method to solve this problem. This finite element analysis is able to analyze stably the limit condition of sheet pile until the back ground of the sheet pile collapse (Tanaka and Okajima, 2001). In this study Mohr-Coulomb type yield function and Drucker-Prager type plastic potential were applied to the constitutive equation.

We investigated also the connecting condition of sheet piles and the function of struts. The stiffness of sheet piles was estimated by modeling the condition of connection. The working effect of struts was estimated by changing the Young's modulus. The soil property was estimated by changing soil cohesions.

2 CONSTITUTIVE EQUATION OF THE FEM

The finite element analysis employed perfect elasto-plastic constitutive equations with a non-associated flow rule. The constitutive equations based on the yield function of Mohr-Coulomb with the plastic potential function of Drucker-Prager are

applied. The finite element is a pseudo-equilibrium model by one-point integration of a 4-node Lagrange-type element. The dynamic relaxation method combined with the generalized return-mapping algorithm is applied to the integration algorithms of elasto-plastic constitutive relations including the effect of the shear banding. This dynamic relaxation method achieves better convergence than the conventional modified Newton-Raphson method.

The yield function (f) and the plastic potential function (Φ) are given by

$$f = \alpha I_1 + \frac{\bar{\sigma}}{g(\theta_L)} - K = 0 \tag{1}$$

$$\Phi = \alpha' I_1 + \bar{\sigma} - K = 0 \tag{2}$$

where

$$\alpha = \frac{2\sin\phi}{\sqrt{3}(3-\sin\phi)} \tag{3}$$

$$\alpha' = \frac{2\sin\psi}{\sqrt{3}(3-\sin\psi)} \tag{4}$$

where I_1 is the first invariant (positive in tension) of deviatoric stresses and $\bar{\sigma}$ is the second invariant of deviatoric stress. With the Mohr-Coulomb model, $g(\theta_L)$ takes the following form.

$$g(\theta_L) = \frac{3-\sin\phi}{2\sqrt{3}\cos\theta_L - 2\sin\theta_L \sin\phi} \tag{5}$$

ϕ is the mobilized friction angle and θ_L is the Lode angle. The frictional hardening-softening functions expressed as follows are used.

The dynamic relaxation method employed in this analysis is the implicit-explicit type. The explicit method without stiffness matrix is applied to the sand mass and the implicit algorithm is applied to a part of the rigid retaining structure, therefore two algorithms are used simultaneously. The algorithms, which used the Newmark scheme are described below.

$$\tilde{q}_{n+1} = q_n + \Delta t v_n + \Delta t^2 (1-2\beta) a_n / 2 \tag{6}$$

$$\tilde{v}_{n+1} = v_n + \Delta t (1-\gamma) a_n \tag{7}$$

Where q_n = displacement vector, v_n = velocity vector, a_n = acceleration vector, Δt =time increment, and γ, β = constant. In a time increment, the displacement (Δq) is simultaneously solved from explicit and implicit effective stiffness matrix using Skyline solver:

Implicit type:

$$K^* = M/(\Delta t^2 \beta) + \gamma C_T/(\Delta t \beta) + K_T(\tilde{q}_{n+1}) \tag{8}$$

Explicit type:

$$K^* = M/(\Delta t^2 \beta) \tag{9}$$

$$K^* \Delta q = \Psi \tag{10}$$

where M = lamp mass, K_T = tangential stiffness matrix, C_T = damping matrix, and Ψ = residual force. This residual force (Ψ) is evaluated by the equation:

$$\Psi = f_{n+1} - Ma_{n+1} - p(\tilde{q}_{n+1}, \tilde{v}_{n+1}) \tag{11}$$

where f_{n+1}=external force vector, and p = internal force vector. The displacement, velocity and acceleration of next step are calculated by following equations.

$$q_{n+1} = \tilde{q}_{n+1} + \Delta q \tag{12}$$

$$a_{n+1} = (q_{n+1} - \tilde{q}_{n+1})/(\Delta t^2 \beta) \tag{13}$$

$$v_{n+1} = \tilde{v}_{n+1} = \Delta t \gamma a_{n+1} \tag{14}$$

3 FEM MESH AND EXCAVATION ANALYSIS

3.1 *Layout of the test pit work*

The test pit was about 13m width and 12m depth as shown Fig. 1. The sheet piles of which penetration depth was 22m were installed. Three struts were installed at 1.5m, 3m and 6m depth. Though the layer from 12m to 14m depth is jet-grouting layer, we did not take into account the effect of jet-grouting in this study.

3.2 *Finite element mesh*

Fig. 2 shows the layout of the FE mesh of the test pit. The number of node is 4615 and the number of element is 4480. The area for analysis is 32.9m wide and 35m depth including test pit area. There are three struts which were set at 0.5m depth, 3.5m depth and 6.5m depth in test pit area. The excavation analysis was performed by deleting one layer at a time of test pit area of the soil elements from above. The deletion of one layer was regarded as one stage of excavation. Elements in the part of struts were installed after the next deeper layer elements were excavated. Beam elements were applied to elements of the strut. We decided that the length between the vertical boundary and the sheet pile of test pit was 32m. This length is over two times of the excavated depth 12m.

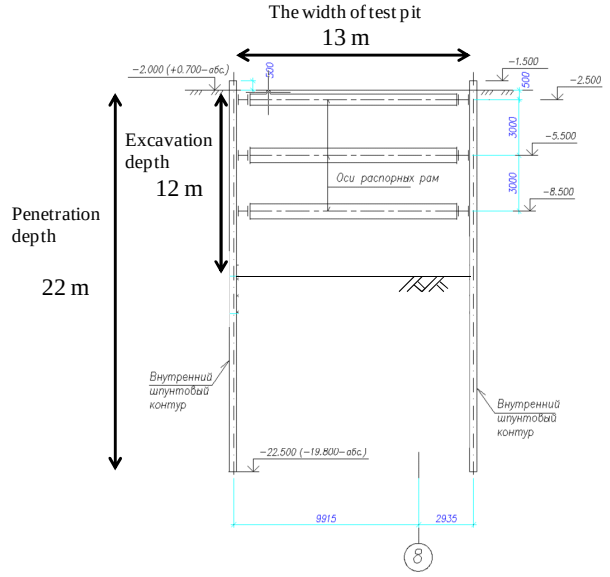

Fig. 1 Layout of the cross section of test pit

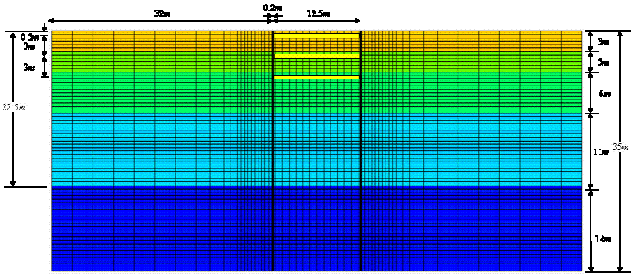

Fig. 2 Layout of FEM mesh and description of modeled soil

3.3 *Figures and photographs*

In this study we assumed that the soils were all cohesive soil (internal friction is zero), and the total stress analysis was applied. The soil parameters that were determined from soil boring log are shown in Fig. 3. The cohesion of soil is estimated by Terzaghi and Peck (1948), (Table 1). We divided the ground to five soil layers as shown in Fig. 3. The shallowest soil layer was from ground level to 3m depth. The cohesion of this soil layer was set to 0.1kgf/cm^2; very soft clay. The secondarily shallower soil layer was from 3m depth to 6m depth. This soil layer cohesion was set to 0.5kgf/cm^2; medium. The third soil layer was from 6m depth to 12m depth. This soil layer cohesion was set to 0.2kgf/cm^2; soft. The fourth soil layer was from 12m depth to 23m depth. This soil layer cohesion was set to 1.0kgf/cm^2; stiff. The deepest soil layer was over 23m depth. This soil layer cohesion was set to 2.0kgf/cm^2; very stiff. Young's modulus of all soil layers was assumed to 50kgf/cm^2. The Poisson's ratio of all layers was assumed to be 0.3.

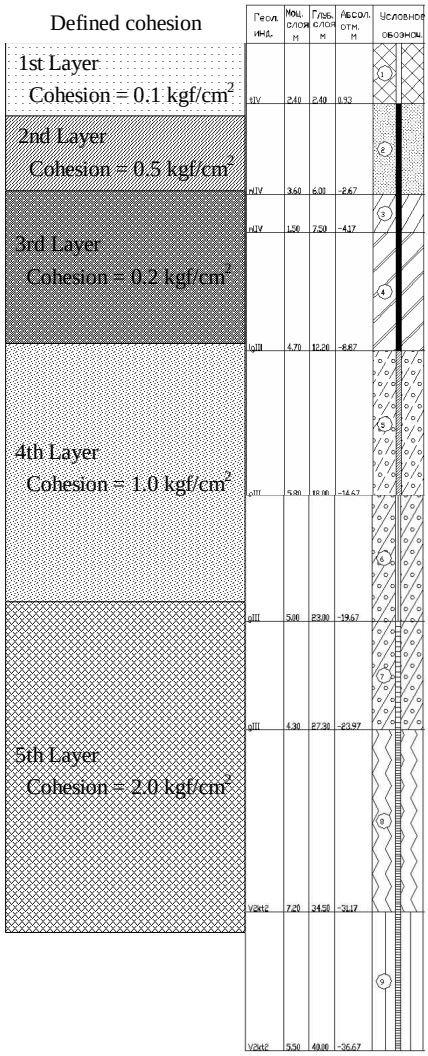

Fig. 3 Geological profile as shown in borehole 4762 and defined cohesion

Table 1 Proposed allowable bearing values for clay

Description of Clay	N	q_u	C
Very soft	Less than 2	Less than 0.27	Less than 0.14
Soft	2 to 4	0.27 to 0.54	0.14 to 0.27
Medium	4 to 8	0.54 to 1.08	0.27 to 0.54
Stiff	8 to 15	1.08 to 2.15	0.54 to 1.08
Very stiff	15 to 30	2.15 to 4.31	1.08 to 2.16
Hard	Over 30	Over 4.31	Over than 2.16

N is number of blows in standard penetration test,
q_u is unconfined compressive strength in kgf par square centimeter,
C is cohesion in kgf par square centimeter

4 MODEL OF STRUCTURE

4.1 *Model of sheet pile condition*

The thickness and the unit weight of elements of the sheet pile were determined in the following way. We regarded the thickness of elements in the part of the sheet pile as the thickness that had the same value as the sheet pile. The Young's modulus

(E) of the sheet pile (L-V) is 2,100,000kgf/cm^2. Here Table2 shows parameters of Larsen piles (CIS standard). The shape of elements in the part of the sheet pile was rectangular solid. When these elements had the same value as the sheet pile, the thickness of sheet pile's elements was calculated from the geometric moment of inertia (I) (shown in Fig. 4). We set two cases. Case 1 has the condition that there is no slippage between piles. In this case the geometric moment of inertia (I) per unit length is 54,000cm^4/m of 1m wall. The thickness of Case1 sheet pile's elements was calculated to be 18.6cm from the geometric moment of inertia (I). The other case (Case 2) has the condition that there is slippage between piles. In this case the geometric moment of inertia (I) per unit length is 15,600cm^4/m that was calculated by 6,243cm^4 (one pile)*1m/0.4m. The thickness of Case2 sheet pile's elements was calculated to be 12.3cm from the geometric moment of inertia (I).

We considered that elements in the part of the sheet pile consisted of sheet pile and the soil. The unit weight per unit square of the sheet pile is 210kgf/m^2 and the area per unit length of the sheet pile (L-V) is 267.6cm^2/m. The unit weight of the soil was regarded as 0.002kgf/cm^3. The unit weight of elements in part of the sheet pile was calculated to be 0.003kgf/cm^3 in the area ratio of the sheet pile and the soil. Sheet pile elements consist of three layers.

4.2 *Model of strut condition*

The Young's modulus and unit weight of elements in the part of strut was determined in the following way. The shape of the strut of test pit was cylinder type in the picture. We assumed that the diameter of the strut was 0.5m, the radial thickness was 0.008m, the material was steel and the strut was located every 4m. We thought that there was the rectangle (12.5m*4m *0.5m) of which the value is equal to the one of a strut. The value of a strut was 5.3*10^8 kgf. The cross section area of the rectangle was 2.0m^2. For these values the Young's modulus was calculated to be 26,000kgf/cm^2. This Young's modulus was applied to the plane strain analysis.

However, the measured horizontal displacement of the sheet piles in the test pit was 12-13cm. This result shows that the effect of struts was little. We computed the excavation works in three patterns which had different Young's modulus 26,000 kgf/cm^2, 2,600kgf/cm^2 and 260kgf/cm^2. For the above we compared "Strut E=26,000kgf/cm^2" as designed condition with the results of test pit work. Then we compared "Strut E=26,000 kgf/cm^2", "Strut E=2,600kgf/cm^2" and "Strut E=260kgf/cm^2" to estimate the effectiveness of strut about Case1 and Case2.

Table 2 Parameters of Larsen piles (CIS standard)

Type	Size of groove, m		Massa 1 running m, kg	Moment of resistance/ moment of inertia, cm^3/ cm^4		Calculation bending moment, kN*m	
	width	height		Grooves	1 m wall	Grooves	1 m wall
L-III	0,4	0,168	62	258/2760	1600/23200	64,5	400
L-IV	0,4	0,18	74	405/4660	2200/39600	101,25	550
L-V	0,4	0,18	100	420/6243	3000/54000	105	750

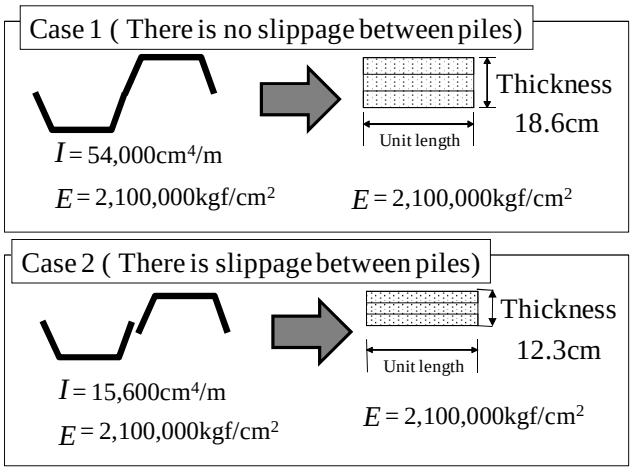

Fig. 4 The modeling of sheet pile

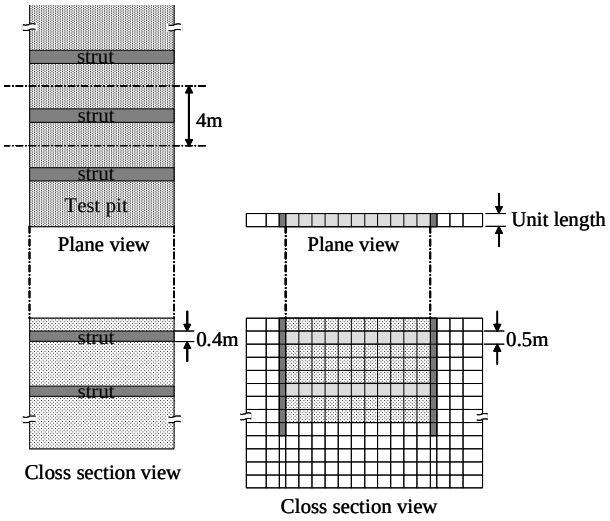

Fig. 5 The picture and modeling of struts

5 RESULTS AND DISCUSSION

We computed the excavation work in different conditions of the strut about Case1 and Case2. Fig.7 shows the comparison of the horizontal displacements of the sheet pile which have different Young's modulus of strut at the last excavation stage (12m depth). We estimated the influence of the strut when the strut Young's modulus had "full": 26,000kgf/cm^2 and "full/10": 2,600kgf/cm^2 and "full/100": 260kgf/cm^2. In the test pit the maximum horizontal displacement was measured about 130mm. In Fig.7 larger displacement of sheet pile was computed in lower strut Young's modulus. Maximum displacements in which the strut has

"full/100": 260kgf/cm^2 were computed to be 115mm in Case1 and 149mm in Case2. However horizontal displacement at the top of the sheet pile in Case1 was larger than one in Case2. Fig.8 indicates that the comparison of the displacement of the sheet pile between the results of FEM of Case1 and Case2 and the results of test pit work at last excavation stage (12m depth). In the test pit work the horizontal displacement at the top of the sheet pile is small (about 30mm). The pattern of displacement of sheet pile Case2 (full/100) is more similar to the test pit work than Case1 (full/100).

From Fig. 7 and Fig.8 it was obvious that the influence of the strut stiffness was larger than the soil condition for the horizontal displacement of the sheet pile in this excavation work. This result shows that there is the possibility that the strut was not fully effective in the test pit work and the sheet piles had some slippage between them.

Next we computed another condition of sheet pile and struts. In the test pit maximum displacement was measured at about 10m depth. We showed a result that this test pit work had forth strut at 9m depth. Fig.9 indicates that the comparison of the displacement which had three struts and the displacement which had forth struts in Case1 (full) at last excavation stage (12m depth). The forth strut had very strong effectiveness to the displacement of the sheet pile. The maximum displacement of sheet pile with 4 struts reduced about half of that with 3 struts. The displacement at the point of third strut and deeper soil layer was greatly reduced. This indicates that the forth strut is effective when large displacement is predicted during the work in a soft clay.

6 CONCLUSION

We analyzed the test pit of the excavation in St. Petersburg soft clay by the elasto-plastic FEM in total stress condition. In the test pit work large displacements of sheet pile were observed. We needed to define many parameters by assumptions because the detailed data were not available. The result of our FEM could show the trend of displacement of the sheet pile observed in the test pit. We estimated that the connecting condition of sheet piles and the working effectiveness of struts by the elasto-plastic FEM. The result shows that there is the possibility that the strut was not fully effective in the test pit work and the sheet piles have slippage between them.

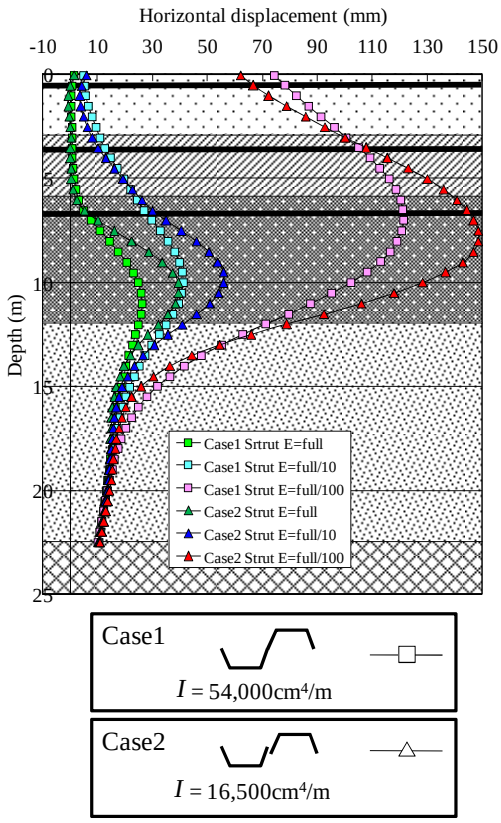

Fig. 7 Comparison of the displacements of the sheet pile which have deferent Young's modulus of strut

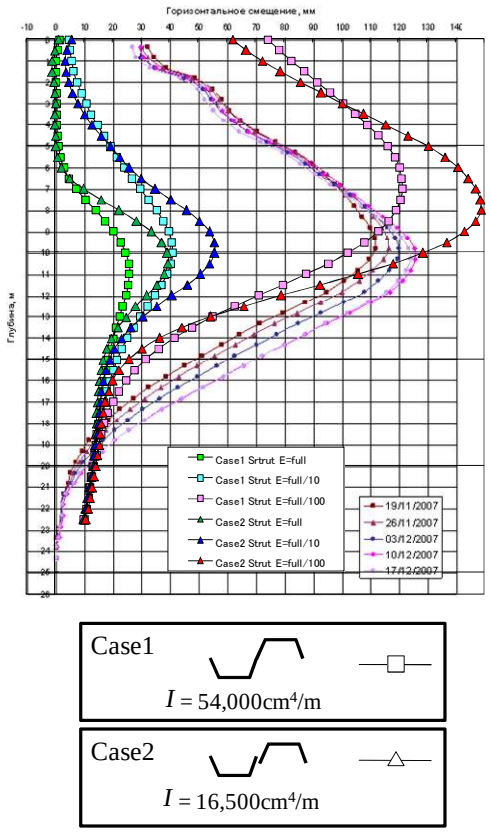

Fig. 8 Comparison of the displacement of the sheet pile between the results of FEM of Case1 and Case2 and the results of test pit work at last excavation stage (12m depth)

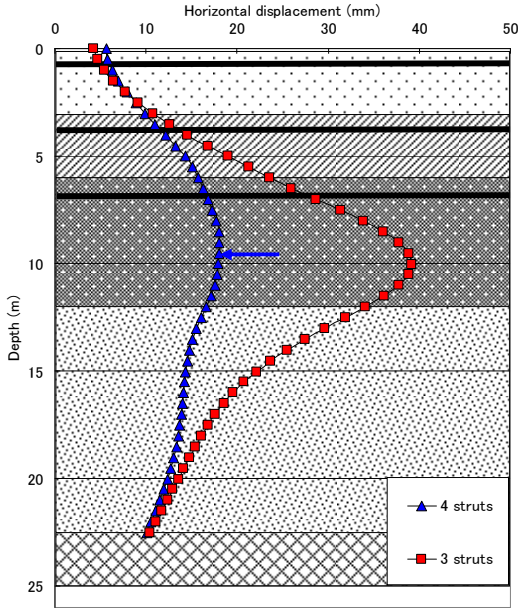

Fig. 9 Comparison of the displacement of the sheet pile which had three struts and the displacement which had four struts at last excavation stage (Case 1)

REFERENCES

Terzaghi, K., and Peck, R.B. (1948). Soil Mechanics in Engineering Practice, John Wiley and Sons

Mori H., and Tanaka T. (2001) "Elasto-plastic finite element analysis of retaining wall with passive mode rotated about the bottom-Infinitesimal deformation analysis and finite deformation analysis." *Computer Methods and Advances in Geomechanics*, Vol.2, 1595-1600

Okajima K., Tanaka T., and Mori H. (2001) "Elasto-plastic finite element collapse analysis of retaining wall by excavation." *Proc. of the First Asian-Pacific Congress on Computational Mechanics* (APCOM'01), Sydney, Vol.1, 439-444

Potts D.M., (2003) "Numerical analysis: a virtual dream or practical reality?" *Geotechnique*, 53-6, 535-573